

RSC Advances



This is an *Accepted Manuscript*, which has been through the Royal Society of Chemistry peer review process and has been accepted for publication.

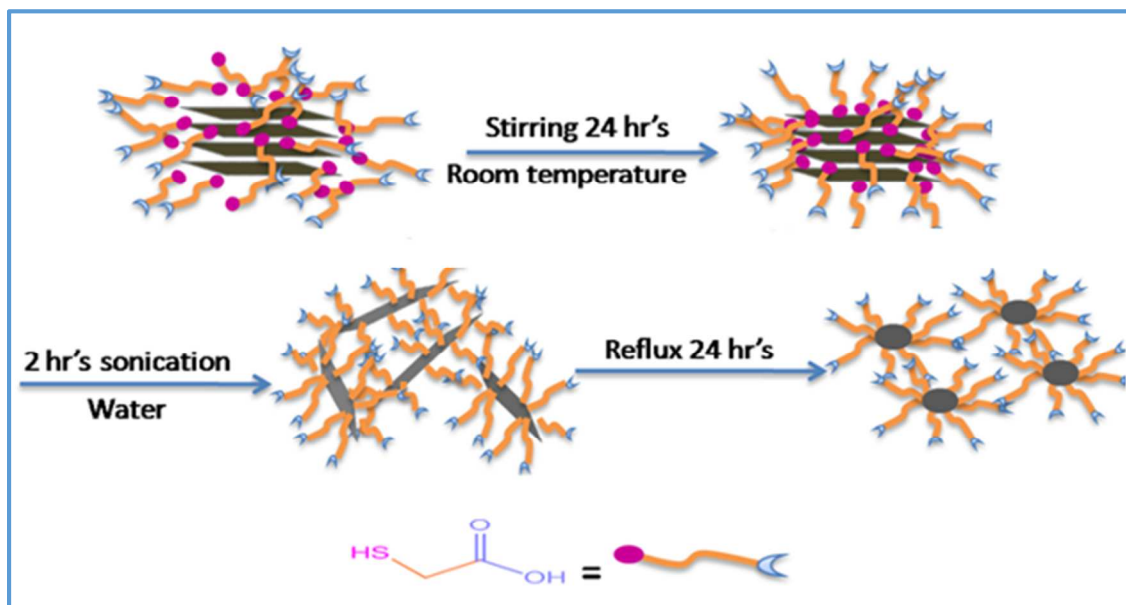
Accepted Manuscripts are published online shortly after acceptance, before technical editing, formatting and proof reading. Using this free service, authors can make their results available to the community, in citable form, before we publish the edited article. This *Accepted Manuscript* will be replaced by the edited, formatted and paginated article as soon as this is available.

You can find more information about *Accepted Manuscripts* in the [Information for Authors](#).

Please note that technical editing may introduce minor changes to the text and/or graphics, which may alter content. The journal's standard [Terms & Conditions](#) and the [Ethical guidelines](#) still apply. In no event shall the Royal Society of Chemistry be held responsible for any errors or omissions in this *Accepted Manuscript* or any consequences arising from the use of any information it contains.

Graphic abstract

Synthesis of water soluble MoS₂ quantum dots from the monolayer nanosheets of MoS₂, using thioglycolic acid (TGA) were reported in this study. TGA molecules not only exfoliated the bulk of MoS₂, but also modified the hydrophobic surface of MoS₂ with hydrophilic carboxylic acid groups.



Highly concentrated MoS₂ nanosheets in water achieved by thioglycolic acid as stabilizer and used as biomarkers

Rajeshkumar Anbazhagan^{1†}, Hsing-Ju Wang^{2†}, Hsieh-Chih Tsai^{1*}, Ru-Jong Jeng^{2*}

1. Graduate Institute of Applied Science and Technology, National Taiwan University of Science and Technology, Taipei, Taiwan

2. Institute Polymer Science and Engineering, National Taiwan University, Taipei, Taiwan.

[†] These authors contributed equally.

[*] To whom correspondence and reprint requests should be addressed.

Prof. Hsieh-Chih Tsai

Email: h.c.tsai@mail.ntust.edu.tw

Tel: +886-2-27303779

Prof. Ru-Jong Jeng

Email: rujong@ntu.edu.tw

Tel: +886-2-33665884

Abstract:

In this work, we reported the synthesis of water soluble MoS₂ quantum dots from the monolayer nanosheets of MoS₂, using thioglycolic acid (TGA) with sonication method. The gaps of MoS₂ layers were enlarged by the stirring process. Meanwhile TGA molecules strongly binding to the defect sites of MoS₂ would reduce the Vander Waals force between the MoS₂ layers through sonication. This led to the improved dispersion of MoS₂ monolayers in water. The addition of TGA molecules not only exfoliated the bulk of MoS₂, but also modified the surface of MoS₂ with carboxylic acid groups. As a result, highly concentrated MoS₂ nanosheets were produced in water. Subsequently, heavy metal-free MoS₂ quantum dots with sustained fluorescence emission, which were fabricated from hydrothermal treatment of MoS₂ mono-layers, can be utilized as cell biomarker.

Introduction:

Since the discovery of graphene, the two dimensional inorganic materials like transition metal dichalcogenides (MoS_2 , MoSe_2 and WS_2) have attracted great attention, particularly molybdenum disulphide (MoS_2) is of great interest in the areas of catalysis,¹ nanotribology,² optical³ and energy storage.⁴ MoS_2 nanomaterials exhibit unique properties such as large intrinsic band gap and high carrier mobility ($1\text{-}40\text{ cm}^2/\text{V.s}$) when exfoliated as monolayers. Bulk MoS_2 have band gap about 1.2 eV. When it became monolayer, the band gap increased to 1.9 eV. The monolayers of MoS_2 possessing strong photoluminescence can be applied as photothermal agents⁵, bio-sensor⁶ and drug carrier.⁷ The MoS_2 monolayers also have a very high surface to mass ratio with ultrathin structure. The large surface to mass ratio creates the possibility of loading a large amount of drug. When compared to the MoS_2 multilayer, the MoS_2 monolayer possesses a higher luminescent efficiency. The luminescent efficiency increases with decreasing layer number.⁸ In addition, MoS_2 quantum dots ($\text{MoS}_2\text{-QD}$) can be obtained when the sizes of exfoliated MoS_2 monolayers are controlled to be less than 100 nm. This would induce the quantum confinement effect of MoS_2 monolayers, leading to photoluminescence emission.⁹ In cell or tissue bioimaging experiment, it requires the use of dye-containing particles for entering cells. Because of this, the particle sizes should be in nanometer (less than 100 nm).¹⁰ For example, in in-vivo experiment, the particle size is more critical and preferably less than 100 nm to avoid the capture by the reticuloendothelial system. Despite some successes in the synthesis of MoS_2 quantum dots,¹¹ these methodologies have limitations to be overcome. The production of MoS_2 quantum dots is typically based on bi- or multi-layer MoS_2 precursors. Furthermore, excessive layer aggregation of MoS_2 would further reduce the photoluminescence properties of MoS_2 . For the preparation of highly photoluminescent $\text{MoS}_2\text{-QD}$, the exfoliation of bulk MoS_2 into monolayer nanosheets is an important step.

Several approaches had been attempted to produce the monolayer nanosheets. A micromechanical cleavage was reported to produce high quality monolayers with low yields.¹² Moreover, liquid-phase exfoliation is one of the most widely used methods to achieve moderate yields.¹³ However; this process requires hazardous organic solvents and a long sonication time. Apart from that, ion intercalation method is also effective in preparing MoS₂ monolayers, but these monolayers tend to comprise metallic MoS₂.⁸ This is inappropriate for a range of applications such as, drug carrier, bio-probe, etc. MoS₂ monolayers can also be achieved by hydrothermal exfoliation, but the issues of high temperature and oxygen sensitivity require special attention.¹⁴ In addition, surfactants are often used to exfoliate the two dimensional materials, owing to the presence of Vander Waals binding and electrostatic stabilization.¹⁵ Although the hydrophobic nature of bulk MoS₂ can be tuned through the surfactant exfoliation, the colloid stability of surfactant-exfoliated MoS₂ still presents a challenge to be solved.¹⁶ In fact, chemically reactive sites are present on the surface of bulk MoS₂ (particularly sulphur vacancy).¹⁷ The number of reactive sites would further increase when bulk MoS₂ are exfoliated to few layers or monolayers. The high molecular affinity of their active sites on MoS₂ has attracted great attention.¹⁸ Because of the surface versatility on MoS₂, one can introduce various functionalization strategies accompanied with exfoliation process to obtain well dispersed MoS₂ monolayers in different solvents (including water). Based on the above, effective exfoliation and chemical functionalization of MoS₂ monolayers would be advantageous and innovative for bio-applications.

In this paper, we report that concurrent liquid-phase exfoliation and functionalization of MoS₂ was successfully achieved using thioglycolic acid (TGA) as an efficient bi-functional ligand.¹⁹ TGA plays the role as an exfoliation ligand to produce nanosheets. Moreover, TGA would link to MoS₂ via thiol chemistry with carboxylic acid end-groups which are supposed to convert hydrophobic nanosheets into hydrophilic ones in an aqueous solution. To the best of our knowledge, this is the first work presenting the exfoliation of MoS₂ in water and subsequent preparation of water soluble

MoS₂-QD. MoS₂-QD is highly potential for bioimaging applications due to its hydrophilic functional groups with bio-compatibility and the quantum confinement effect with fluorescence characteristics.

Before the addition of TGA to the water-MoS₂ system, the MoS₂ was insoluble due to its hydrophobic nature. However, after the addition of TGA to the water-MoS₂ system, the MoS₂ monolayers became soluble (hydrophilic) and were well suspended in water because the hydrophobic surface of MoS₂ was covered with acid (COOH) end group of TGA (Figure 1a). The large amount of well-suspended MoS₂ monolayers in water was prepared by stirring at room temperature and simple ultra-sonication. Infrared spectroscopy was used to identify the structure of MoS₂ with the addition of TGA. The presence of carbonyl and hydroxyl peaks at 1713 and 3400 cm⁻¹, respectively, and the disappearance of thiol peak at 2561 cm⁻¹ indicate that the surface of MoS₂ was successfully modified with TGA (Figure 1b). The prepared MoS₂ was further analyzed by UV-visible spectroscopy. The UV-visible absorption spectrum of a dilute modified MoS₂ solution rendered a peak at 420 nm⁻¹ owing to convoluted excitonic peaks while the peaks emerged from the k point of Brillouin zone were observed at 620 and 670 nm⁻¹. This result indicates that these suspended MoS₂ monolayers exhibited pristine semiconductor 2H-MoS₂ phase unlike the ones from the ion intercalation method (Figure 1c).¹³ It is important to note that a high yield of MoS₂ nanosheets could also be achieved in this work as confirmed by UV spectroscopy. The mass of MoS₂ monolayer in the water solution (after dialysis) allows one to define the yields of MoS₂ monolayers. The concentration (yield) of exfoliated MoS₂ monolayers was 3.49 mg/mL in water. In fact, the concentration of MoS₂ monolayers would increase with increasing sonication time (Supporting Information). The colloidal stability of dispersion was investigated by measuring zeta potential. The values (-88 mV for pristine MoS₂ and -47 mV for TGA-modified MoS₂) of MoS₂ implies that the surface of MoS₂ was successfully modified by TGA (Figure-1d). This is consistent with the result

reported in literature.²⁰ Moreover, the colloidal stability of TGA-MoS₂ was evaluated for more than 3 months; TGA-MoS₂ monolayers remained well dispersed afterwards.

In Raman spectrum of bulk MoS₂, a notable in-plane (E_{2g}^1) peak at 383 cm⁻¹ and an out-plane peak (A_{1g}) at 407 cm⁻¹ were observed. The former one is due to in-plane sulphur molybdenum vibration and the later one is due to out-plane sulphur vibrations. As MoS₂ was exfoliated to monolayers, the frequency of in-plane mode increased and frequency of out-plane mode decreased. The gap between the frequencies of in-plane and out-plane modes depends on the method of exfoliation. A closing gap implies that the monolayer structure is more predominant. In the exfoliated TGA-MoS₂ monolayers, in-plane and out-plane peaks were observed at 385 cm⁻¹ and 406 cm⁻¹, respectively (Figure 1e). This indicates the presence of MoS₂ monolayer and few-layer structure.²¹ The gap of E_{2g}^1 , A_{1g} peaks in Figure 2a was somewhat broadening when compared to those of the mechanically exfoliated molybdenum disulphide monolayers.²² This might be due to the larger thicknesses of MoS₂ monolayers caused by the presence of TGA on the surfaces. XRD was used to identify the crystal structure of the exfoliated MoS₂ monolayers. The pristine molybdenite showed a very sharp peak at 14.8° (002), and peaks with lower intensity at 39.5° (103) and 49.8° (105). The XRD pattern of exfoliated MoS₂ monolayers displayed a peak only at 14.8° corresponding to the (002) plane of 2H-MoS₂. In addition, the absence of (001) peak at 32.8° indicates that the majority of exfoliated dispersions exhibited the single-layer nanosheets (Figure 1f).²³

The morphology of the functionalized MoS₂ was investigated by TEM. The results indicate the lengths of the nanosheets ranged from 100 to 500 nm. Moreover, most of the nanosheets were transparent to the electron beam (Figure 2a). This is because of the ultrathin structure of exfoliated MoS₂ monolayers. The electron diffraction pattern of the TEM image was utilized to confirm the symmetry of the exfoliated materials, indicating that each molybdenum disulphide monolayer retained its hexagonal symmetry just like bulk MoS₂ crystals (Figure 2b). These exfoliated materials

possessing a honeycomb-like structure without any defects was observed in a HR-TEM image (inset image of Figure 2b).²⁴ In addition, a large number of nanosheets deposited in the holey carbon grid were also observed in Figure 2c. TEM results imply that TGA played the role of a ligand for the effective exfoliation of MoS₂. It is noteworthy that a robust and high yield production of MoS₂ monolayers could be achieved via the thiol chemistry between TGA and MoS₂. An AFM image of the TGA-MoS₂ nanosheets is shown in Figure 2d. The topographic height of the exfoliated MoS₂ material was around 1 nm (Figure 2e), indicating the presence of monolayers. Figure 2f illustrates the size distribution of the quantum dots. The prepared MoS₂-QD exhibited sizes ranged from 5 to 10 nm (the average diameter range is about 7 nm).

Due to the excellent optoelectronic properties of two-dimensional MoS₂ nanomaterials, we first set out to explore the possibility of MoS₂-QD bio-probe for human HeLa cancer cells. Figure 3a presents the fluorescence spectrum of the MoS₂-QD and the absorption spectrum was shown in the Figure 3b. Different fluorescence emissions normally depend on the particle size of the quantum dot. This result implies the prepared MoS₂-QD also exhibited polydispersity.⁸ The fluorescence emissions of the prepared quantum dots started from an excitation wavelength at 350 to 430 nm. In addition, the maximum fluorescence wavelength was around 440 nm with an excitation wavelength of 360 nm. The figure 3c shows the photograph of MoS₂-QD the visible and UV light. MoS₂-QD uptake and bio-imaging application were investigated by a confocal fluorescence microscope. The confocal image of MoS₂-QD internalized by HeLa cells was observed in Figure 3d, 3e and 3f. The presence of the blue color in the region inside the HeLa cell indicates the successful uptake of MoS₂-QD through the cell membrane. Furthermore, MoS₂-QD exhibited impressive biocompatible properties given the fact that the HeLa cell remained alive with the addition of MoS₂-QD. This result implies that MoS₂-QD could be biocompatible, used as biomarker and some other biomedical applications.

Conclusion

An effective exfoliation process of MoS₂ into single layer nanosheets with high yields has been developed in this work. In this process, TGA not only played the role of an exfoliation ligand to produce MoS₂ monolayers, but also linked to MoS₂ via thiol chemistry with carboxylic acid end-groups. Because of this, bulk MoS₂ could be exfoliated in water and subsequent preparation of water soluble MoS₂-QD. Due to the low cytotoxicity and excellent biocompatibility, MoS₂-QD was demonstrated to be an eco-friendly material as well as a biolabeling agent.

Experimental Section

Preparation of MoS₂ nanosheet:

In a typical experiment, 1.86 gram of TGA and 400 mg of molybdenum disulphide were placed (the optimization concentration of TGA for this reaction was added in Supporting Information) in a 25 ml glass vial. The reaction mixture was then stirred for 24 h. Subsequently 20 ml of fresh water was added to the reaction mixture, which was sonicated for 2 h (Sonicator: DELTA, DC400H, 400W). After sonication, the reaction mixture was centrifuged at the speed of 1500 rpm to remove undesirable aggregated materials. The supernatant was collected and placed in the dialysis membrane. Dialysis was performed for 48 h to remove the excess of TGA with a cut-off molecular weight at 1000 Da.

Preparation of MoS₂ quantum dot:

MoS₂-QD was prepared by refluxing of MoS₂ monolayers in water for 24 h.⁸ The resulting reaction mixture was filtered off using a 0.43 micrometer membrane filter, and then a transparent MoS₂-QD solution was obtained.

Internalization:

MoS₂-QD internalized by HeLa cells were visualized using an LTCS SP5 confocal spectral microscopy imaging system (Leica Microsystems, Wetzlar, Germany). HeLa cells were cultured on cover slides for 24 h and treated with MoS₂-QD. The concentration of MoS₂-QD was fixed at 1 μg/mL. After 2 h of incubation, cells were washed with a phosphate buffer solution and mounted on a slide with 4% w/w paraformaldehyde for confocal observation. Fluorescence was observed by confocal microscopy using 360 nm excitation and a long-pass filter of either 450 nm for MoS₂-QD detection.

Acknowledgements

The authors would like to thank Ministry of Science and Technology, Taiwan for financial support (NSC 100-2221-E-007-011-030-MY3).

Reference:

- 1 Karunadasa, H. I. Montalvo, E. Sun, Y. Majda, M. Long, J.R. Chang, J. Christopher Science 2012, 335, 698.
- 2 J. J. Hu, J. S. Zabinski Tribol. Lett. 2005, 18, 173.
- 3 D. Sercombe; D. Schwarz, O.D. Pozo-Zamudio, F. Liu, B.J. Robinson, E.A. Chekhovich, I. I. Tartakovskii, O. Kolosov, A.I. Tartakovskii Sci. Rep. 2013, 3.
- 4 T. Stephenson, Z. Li, B. Olsen, D. Mitlin Energy Environ. Sci. 2014, 7, 209.
- 5 S. S. Chou, B. Kaehr, J. Kim, B. M. Foley, M. De, P. E. Hopkins, J. Huang, C.J. Brinker, V.P. Dravid Angew. Chem.Int.Ed. 2013, 52, 4160.
- 6 S. Wu, Z. Zeng, H. Qiyuan, Z. Wang, S.J. Wang, Y. Du, Z. Yin, X. Sun, W. Chen, H. Zhang Small 2012, 8, 2264.

- 7 T. Liu, C. Wang, X. Gu. H. Gong, L. Cheng, X. Shi, L. Feng, B. Sun, Z. Liu *Adv.Mater.* 2014, 26, 3433.
- 8 G. Eda; H. Yamaguchi, D. Voiry, T. Fujita, M. Chen, M. Chhowalla *Nano Lett.* 2011, 11, 5111.
- 9 V. Stengl, J. Henych *Nanoscale* 2013, 5, 3387.
- 10 S. Zhu , J. Zhang , C. Qiao, S. Tang, Y. Li , W. Yuan, B. Li, L. Tian, F. Liu, R. Hu, H. Gao, H. Wei, H. Zhang, H. Sun and B. Yang *Chem. Commun.* 2011, 47, 6858.
- 11 D. Gopalakrishnan, D. Damien, M. M. Shaijumon *ACS Nano* 2014, 8, 5297.
- 12 Z. Yin, H. Li, H. Li, L. Jiang, Y. Shi, Y. Sun, G. Lu, Q. Zhang, X. Chen, H. Zhang *ACS Nano* 2011, 6, 74.
- 13 A. O'Neill, U. Khan, J.N. Coleman *Chem. Mater.* 2012, 24, 2414.
- 14 K. K. Liu, W. Zhang, Y. H. Lee, Y. C. Lin, M. T. Chang, C. Y. Su, C. S. Chang, H. Li, Y. Shi, H. Zhang, C. S. Lai, L. J. Li *Nano Lett.* 2012, 12, 1538.
- 15 R. J. Smith, P. J. King, M. Lotya, C. Wirtz, U. Khan, S. De, A. O'Neill, G. S. Duesberg, J.C. Grunlan, G. Moriarty, J. Chen, J. Wang, A. I. Minett, V. Nicolosi, J. N. Coleman *Adv.Mater.* 2011, 23, 3944.
- 16 S. D. Jiang, G. Tang, Z. M. Bai, Y. Y. Wang, Y. Hu, L. Song *RSC Adv.* 2014, 4, 3253.
- 17 T. F. Jaramillo, K. P. Jørgensen, J. Bonde, J. H. Nielsen, S. Horch, Ib. Chorkendorff *Science* 2007. 317, 100.
- 18 J. A. Spirko, M. L. Neiman, A. M. Oelker, K. Klier *Surface Science* 2004. 572, 191.
- 19 C. Altavilla, M. Sarno, P. Ciambelli *Chem. Mater.*, 2011, 23, 3879.
- 20 S. S. Chou, M. De, J. Kim, S. Byun, C. Dykstra, J. Yu, J. Huang, V. P. Dravid *J. Am. Chem. Soc.* 2013. 135, 4584.
- 21 C. Lee, H. Yan, L. E. Brus, T. F. Heinz, J. Hone, S. Ryu *ACS Nano* 2010, 4, 2695.
- 22 T. S. Sreeprasad, P. Nguyen, N. Kim, V. Berry *Nano Lett.* 2013. 13, 4434.

23 C. F. Castro-Guerrero, F. L. Deepak, A. Ponce, J. C. Reyes, M. D. Valle-Granados, S. F. Moyado, D. H. Galvan, M. J. Yacamán *Catal. Sci. Technol.* 2011. 1, 1024.

24 Y. Yao, L. Tolentino, Z. Yang, X. Song, W. Zhang, Y. Chen, J. P. Wong *Advanced Functional Materials* 2013. 23, 3577.

Figure caption:

Figure 1(a) Photograph of prepared MoS₂ nanosheet dispersion in water (Left is without TGA and Right is with TGA). (b) Infrared spectrum of pristine MoS₂, TGA-MoS₂ monolayers and TGA. (c) UV-visible spectrum of TGA-MoS₂ monolayers at various TGA concentration (d) Zeta potential values of pristine MoS₂ and TGA-MoS₂ monolayers. (e) Raman spectrum of pristine MoS₂ and TGA-MoS₂ monolayers. (f) XRD spectrum of pristine MoS₂ and TGA-MoS₂.

Figure 2(a) TEM image of TGA-MoS₂ monolayers deposited on holey carbon grid. (b) Electron diffraction pattern of exfoliated MoS₂ nanosheet from the image of (a). The inset image of figure (b) shows the honeycomb arrangement of exfoliated TGA-MoS₂ monolayers. (c) The high yields of MoS₂ monolayers deposited on TEM grid. (d) And (e) AFM image and height profile of TGA-MoS₂ monolayers. (f) TEM image of prepared quantum dots.

Figure 3(a) Normalized fluorescence spectrum of MoS₂-QD with different excited wavelength. (b) UV-Visible spectrum of MoS₂-QD. (c) photograph of MoS₂-QD under visible and UV light. (d) Bright field image of quantum dot with cells. (e) Fluorescence image of quantum dot with cells. (f) Merged image of fluorescence and bright field with HeLa cells.

Figure 1

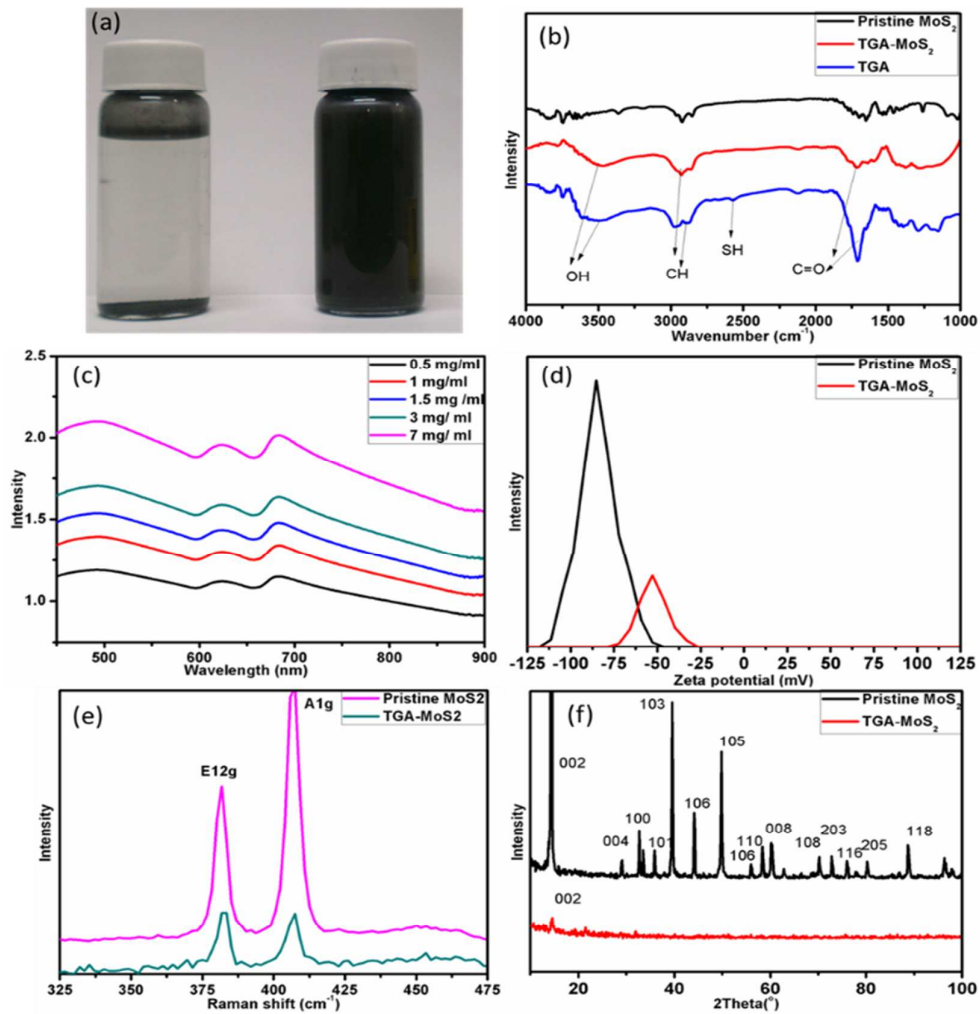


Figure 2

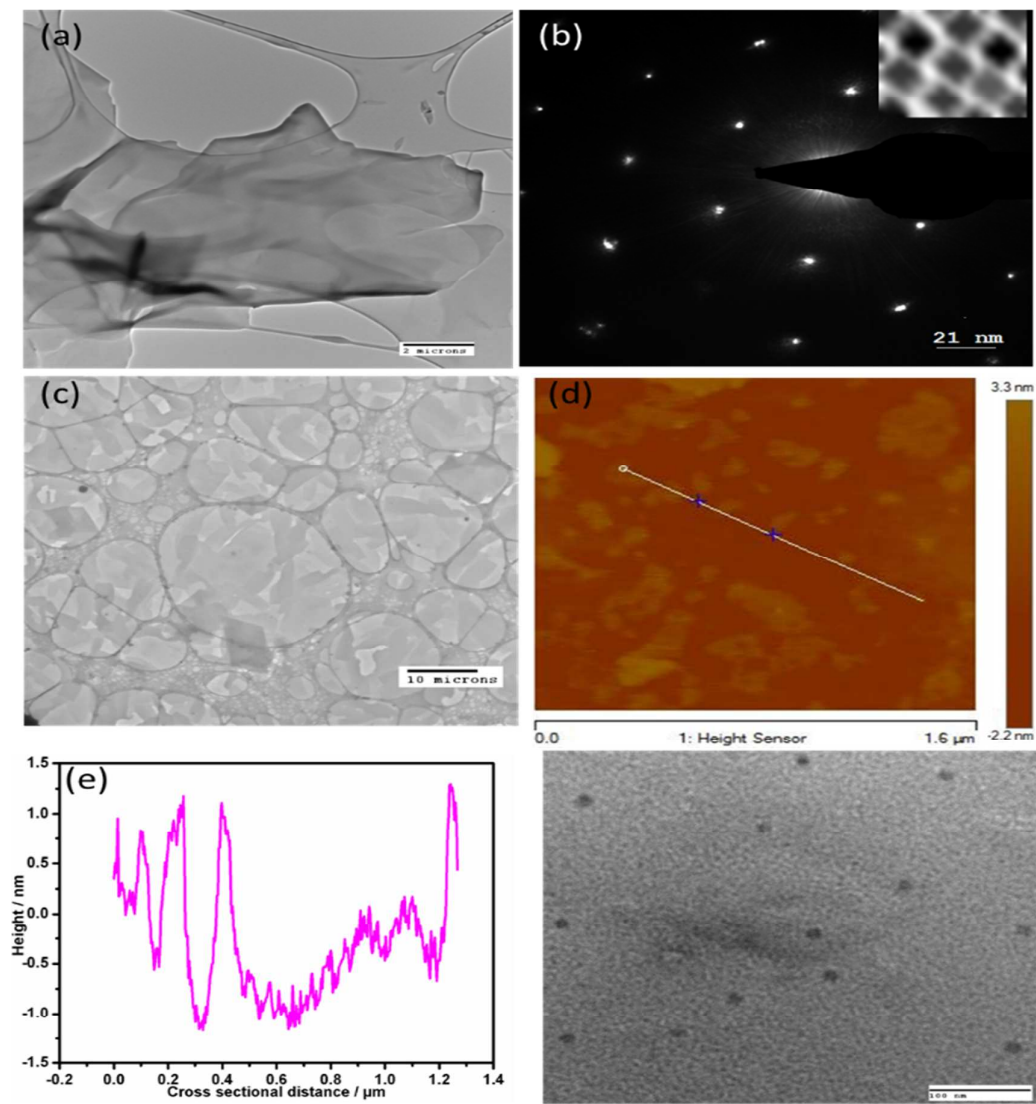


Figure 3

